



Sandia
National
Laboratories

SAND2024-09364C

Mesh Optimization and Basis Compression for Extreme-Scale Solution of Partial Differential Equations

Graham Harper, Denis Ridzal, Tim Wildey
Center for Computing Research, Sandia National Laboratories

WCCM 2024

July 22, 2024

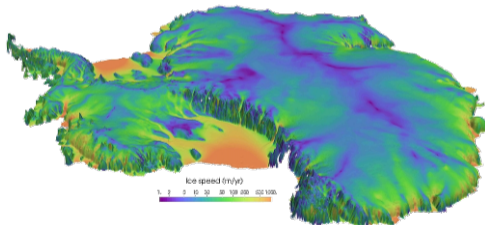
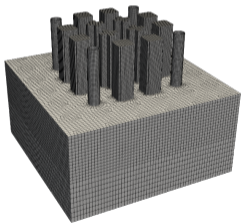


Sandia National Laboratories is a
multimission laboratory managed
and operated by National Technology
& Engineering Solutions of Sandia,
LLC, a wholly owned subsidiary of
Honeywell International Inc., for the
U.S. Department of Energy's National
Nuclear Security Administration under
contract DE-NA0003525.

SAND2024-09364C

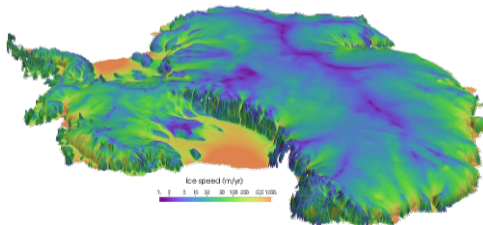
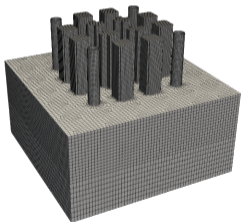
2 Motivation

- Modern computing technologies (accelerators, edge, etc.) have **less memory bandwidth**.
- Supercomputing post-Moore's Law cannot rely on flops alone.
- Computations with less data can **save compute time and reduce memory overhead**.
- Mathematical structure in finite element methods (FEMs) can be exploited.



2 Motivation

- Modern computing technologies (accelerators, edge, etc.) have **less memory bandwidth**.
- Supercomputing post-Moore's Law cannot rely on flops alone.
- Computations with less data can **save compute time and reduce memory overhead**.
- Mathematical structure in finite element methods (FEMs) can be exploited.



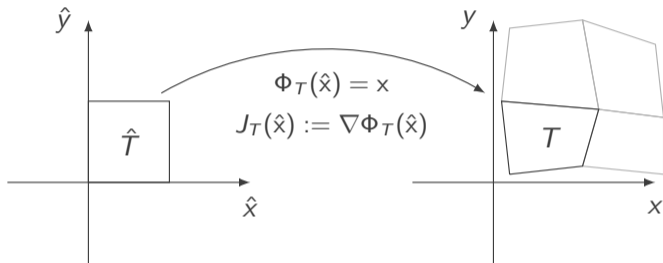
Two main goals of this talk:

- Detection and exploitation of structure in FEM computations
- Enhancement of structure for FEM computations

3 Reference to Physical Mapping



The most important tool for evaluating FEM integrals is the **reference to physical mapping**.

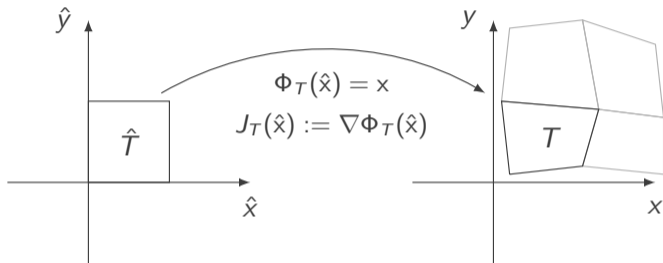


The reference to physical mapping Φ_T for a mesh cell T and reference cell \hat{T} , which relates a function $\hat{f}(\hat{x})$ with $f(x)$ by $f(x) = \hat{f}(\Phi_T^{-1}(x))$

3 Reference to Physical Mapping



The most important tool for evaluating FEM integrals is the **reference to physical mapping**.



The reference to physical mapping Φ_T for a mesh cell T and reference cell \hat{T} , which relates a function $\hat{f}(\hat{x})$ with $f(x)$ by $f(x) = \hat{f}(\Phi_T^{-1}(x))$

Oftentimes, such FEM assembly calculations scale like

$$\mathcal{O}(N(p+1)^d q^d d) \quad (1)$$

Our target is the term in red.

4 Finite Element Operator Assembly



Main computation: **integrals**

From calculus,

$$\int_T f(x) dx = \int_{\hat{T}} \hat{f}(\hat{x}) \det(J_T(\hat{x})) d\hat{x}. \quad (2)$$

4 Finite Element Operator Assembly



Main computation: **integrals**

From calculus,

$$\int_T f(\mathbf{x}) \, d\mathbf{x} = \int_{\hat{T}} \hat{f}(\hat{\mathbf{x}}) \det(J_T(\hat{\mathbf{x}})) \, d\hat{\mathbf{x}}. \quad (2)$$

From differential geometry,

$$\int_T \nabla f(\mathbf{x}) \, d\mathbf{x} = \int_{\hat{T}} J_T^{-T}(\hat{\mathbf{x}}) \nabla \hat{f}(\hat{\mathbf{x}}) \det(J_T(\hat{\mathbf{x}})) \, d\hat{\mathbf{x}}. \quad (3)$$

4 Finite Element Operator Assembly



Main computation: **integrals**

From calculus,

$$\int_T f(x) dx = \int_{\hat{T}} \hat{f}(\hat{x}) \det(J_T(\hat{x})) d\hat{x}. \quad (2)$$

From differential geometry,

$$\int_T \nabla f(x) dx = \int_{\hat{T}} J_T^{-T}(\hat{x}) \nabla \hat{f}(\hat{x}) \det(J_T(\hat{x})) d\hat{x}. \quad (3)$$

Unified by the **de Rham complex**,

$$\begin{array}{ccccccc} \text{space:} & HGRAD & \xrightarrow{\nabla} & HCURL & \xrightarrow{\nabla \times} & HDIV & \xrightarrow{\nabla \cdot} & HVOL \\ & H^1(\Omega) & & H(curl, \Omega) & & H(div, \Omega) & & L^2(\Omega) \\ \text{pullback:} & I & & J^{-T} & & J \det(J)^{-1} & & \det(J)^{-1} \end{array}$$

4 Finite Element Operator Assembly



Main computation: **integrals**

From calculus,

$$\int_T f(x) dx = \int_{\hat{T}} \hat{f}(\hat{x}) \det(J_T(\hat{x})) d\hat{x}. \quad (2)$$

From differential geometry,

$$\int_T \nabla f(x) dx = \int_{\hat{T}} J_T^{-T}(\hat{x}) \nabla \hat{f}(\hat{x}) \det(J_T(\hat{x})) d\hat{x}. \quad (3)$$

Unified by the **de Rham complex**,

$$\begin{array}{ccccccc} \text{space:} & HGRAD & \xrightarrow{\nabla} & HCURL & \xrightarrow{\nabla \times} & HDIV & \xrightarrow{\nabla \cdot} & HVOL \\ & H^1(\Omega) & & H(curl, \Omega) & & H(div, \Omega) & & L^2(\Omega) \\ \text{pullback:} & I & & J^{-T} & & J \det(J)^{-1} & & \det(J)^{-1} \end{array}$$

Most importantly, $J_T(\hat{x})$ is **invariant under mesh cell translations**.

5 Finite Element Basis Compression Lemma



Lemma

If two mesh cells T_1 and T_2 are translations of each other, FEM operator assembly satisfies

$$\int_{T_1} \nabla \phi_i(\mathbf{x}) \cdot \nabla \phi_j(\mathbf{x}) \, d\mathbf{x} = \int_{T_2} \nabla \phi_i(\mathbf{x}) \cdot \nabla \phi_j(\mathbf{x}) \, d\mathbf{x} \quad (4)$$

5 Finite Element Basis Compression Lemma



Lemma

If two mesh cells T_1 and T_2 are translations of each other, FEM operator assembly satisfies

$$\int_{T_1} \nabla \phi_i(\mathbf{x}) \cdot \nabla \phi_j(\mathbf{x}) \, d\mathbf{x} = \int_{T_2} \nabla \phi_i(\mathbf{x}) \cdot \nabla \phi_j(\mathbf{x}) \, d\mathbf{x} \quad (4)$$

Proof.

As T_1 and T_2 are translations of each other, we have $J_{T_1} \equiv J_{T_2}$ and

$$\begin{aligned} \int_{T_1} \nabla \phi_i(\mathbf{x}) \cdot \nabla \phi_j(\mathbf{x}) \, d\mathbf{x} &= \int_{\hat{T}} J_{T_1}^{-T}(\hat{\mathbf{x}}) \nabla \hat{\phi}_i(\hat{\mathbf{x}}) \cdot J_{T_1}^{-T}(\hat{\mathbf{x}}) \nabla \hat{\phi}_j(\hat{\mathbf{x}}) \det(J_{T_1}(\hat{\mathbf{x}})) \, d\hat{\mathbf{x}} \\ &= \int_{\hat{T}} J_{T_2}^{-T}(\hat{\mathbf{x}}) \nabla \hat{\phi}_i(\hat{\mathbf{x}}) \cdot J_{T_2}^{-T}(\hat{\mathbf{x}}) \nabla \hat{\phi}_j(\hat{\mathbf{x}}) \det(J_{T_2}(\hat{\mathbf{x}})) \, d\hat{\mathbf{x}} \\ &= \int_{T_2} \nabla \phi_i(\mathbf{x}) \cdot \nabla \phi_j(\mathbf{x}) \, d\mathbf{x} \end{aligned}$$



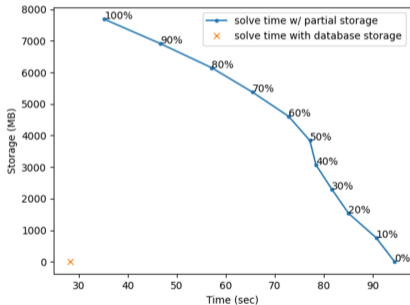
6 Finite Element Basis Compression



- Extension to other operators is a trivial consequence of the de Rham Complex.
- Cell similarity data may be stored with a mesh, costing 1 integer type per cell
- Index basis data by $\text{basis}(i,p,q,d) := \text{basis_ref}(\text{lookup}(i),p,q,d)$

6 Finite Element Basis Compression

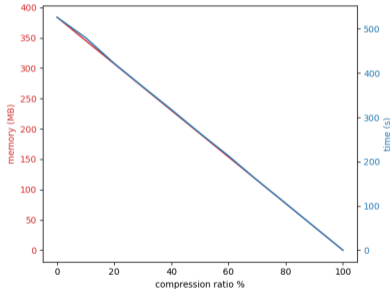
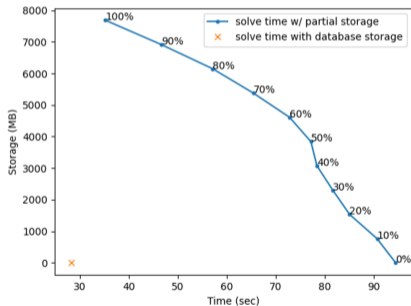
- Extension to other operators is a trivial consequence of the de Rham Complex.
- Cell similarity data may be stored with a mesh, costing 1 integer type per cell
- Index basis data by $\text{basis}(i, p, q, d) := \text{basis_ref}(\text{lookup}(i), p, q, d)$



6 Finite Element Basis Compression



- Extension to other operators is a trivial consequence of the de Rham Complex.
- Cell similarity data may be stored with a mesh, costing 1 integer type per cell
- Index basis data by $\text{basis}(i, p, q, d) := \text{basis_ref}(\text{lookup}(i), p, q, d)$



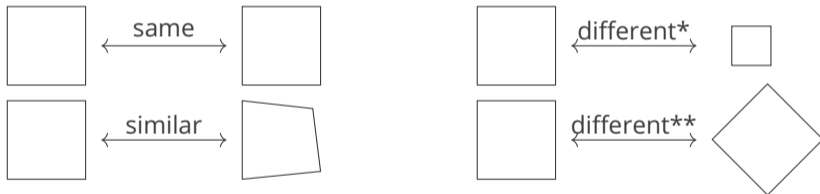
(left) Total time and basis storage costs for partial basis storage on (right) Basis evaluation timings and basis storage costs for compression of one million elements $p = 1, q = 2$ on a 3.00GHz Intel Xeon Gold 6248R.

7 Finite Element Basis Compression



Let $\varepsilon > 0$ be a compression tolerance. Compress functions evaluating

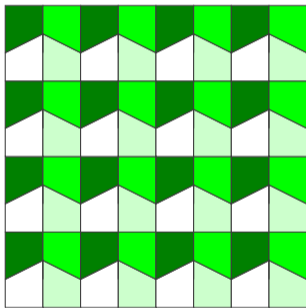
$$d(J_i, J_j) = \int_{\hat{T}} \frac{\|J_i - J_j\|_F}{\|J_i\|_F} d\hat{T}. \quad (5)$$



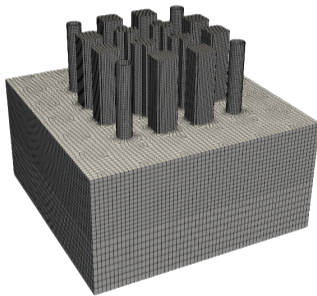
*scalings can be accounted for by a diagonal transform in the de Rham complex, but are beyond current scope

**rotations can be accounted for by a unitary transform in the de Rham complex, but are beyond current scope

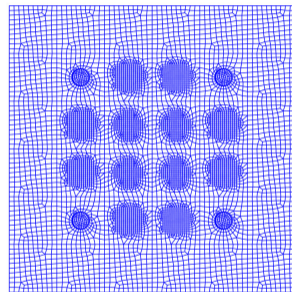
8 Finite Element Basis Compression



93.75% compression



99.9% compression



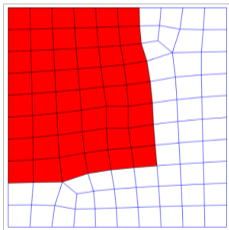
62.52% compression

***Compression is performed on a per-process basis.**

9 R-Adaptive Mesh Optimization



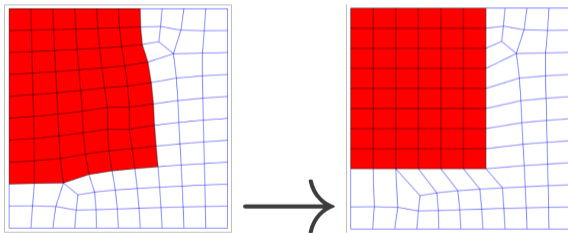
- R-adaptive mesh optimization repositions mesh nodes without touching topology.
- Goal: Enhance the compressible structure in the mesh by optimizing node locations.
- For simplicity, focus on quadrilateral meshes



9 R-Adaptive Mesh Optimization

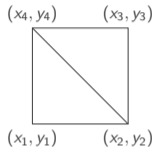
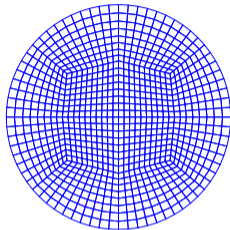


- R-adaptive mesh optimization repositions mesh nodes without touching topology.
- Goal: Enhance the compressible structure in the mesh by optimizing node locations.
- For simplicity, focus on quadrilateral meshes



Example of an r-adaptive mesh modification to enhance basis compression. (left) starting mesh (right) adapted mesh with structured region

- \mathcal{T}_h mesh
- N cells, N_p nodes
- $\hat{p}_i = (x_i, y_i)$, $i = 1, \dots, N_p$ node coordinates
- $\hat{p}_{i,j} = (x_{i,j}, y_{i,j})$, $i = 1, \dots, N$, $j = 1, 2, 3, 4$ is the j th node of cell i
- $J_{T_i}(\hat{x})$, $i = 1, \dots, N$ Jacobian of cell i



- Split T_i into two triangles using nodes 1,2,4 and nodes 3,4,2
- Define $K_i(p)$, $i = 1, \dots, N$ as the combination of the Jacobians from the subtriangles

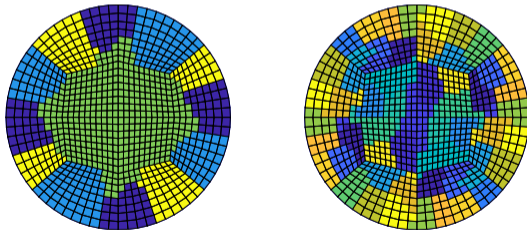
$$K_i(p) = [x_{i,2} - x_{i,1}, x_{i,4} - x_{i,1}, x_{i,4} - x_{i,3}, x_{i,2} - x_{i,3}, y_{i,2} - y_{i,1}, y_{i,4} - y_{i,1}, y_{i,4} - y_{i,3}, y_{i,2} - y_{i,3}] \quad (6)$$

11 Mesh Structure Detection



What defines an “ideal” or “target” shape?

- Perform structure detection on 8-dimensional $K_i(p)$ dataset
- Utilize k -means algorithm and related variants
- Set parameters to minimize cluster variance and “overlap”
- Cluster center for cell i becomes target μ_i



The circle mesh clustered using k -means with 4 and 20 clusters based on cell shapes.

12 Optimization Objective

We want to reduce

$$\|\vec{K}(p) - \vec{\mu}\|_{\ell_0}^2.$$



12 Optimization Objective

We want to reduce

$$\|\vec{K}(\mathbf{p}) - \vec{\mu}\|_{\ell_0}^2.$$

Therefore, we consider reducing

$$\|\vec{K}(\mathbf{p}) - \vec{\mu}\|_{\ell_1}^2. \tag{7}$$

12 Optimization Objective



We want to reduce

$$\|\vec{K}(\mathbf{p}) - \vec{\mu}\|_{\ell_0}^2.$$

Therefore, we consider reducing

$$\|\vec{K}(\mathbf{p}) - \vec{\mu}\|_{\ell_1}^2. \tag{7}$$

Replacing with elastic variables u, v , adding ℓ_2 regularization, we obtain

$$\frac{a}{2} \|(u, v)\|_{\ell_2}^2 + \sum_{i=1}^N \sum_{j=1}^8 u_{i,j} + v_{i,j} \tag{8}$$

subject to

$$K_i(\mathbf{p}) - \mu_i = u_i - v_i, \quad i = 1, \dots, N, \tag{9}$$

$$u_i \geq 0, \quad i = 1, \dots, N, \tag{10}$$

$$v_i \geq 0, \quad i = 1, \dots, N. \tag{11}$$

13 Volume and Feature Preservation Constraints



To protect mesh quality, bound cell volumes

$$v_{i,min} \leq v_i(\mathbf{p}) \leq v_{i,max}, \quad i = 1, \dots, N,$$

where

$$v_i(\mathbf{p}) = \frac{1}{2} \sum_{j=1}^4 x_{i,j+1} y_{i,j} - x_{i,j} y_{i,j+1}, \quad i = 1, \dots, N$$

Volume and Feature Preservation Constraints



To protect mesh quality, bound cell volumes

$$v_{i,min} \leq v_i(\mathbf{p}) \leq v_{i,max}, \quad i = 1, \dots, N,$$

where

$$v_i(\mathbf{p}) = \frac{1}{2} \sum_{j=1}^4 x_{i,j+1} y_{i,j} - x_{i,j} y_{i,j+1}, \quad i = 1, \dots, N$$

Replace cell volumes by slack variables

$$v_i(\mathbf{p}) - s_i = 0, \quad i = 1, \dots, N \tag{12}$$

$$v_{i,min} \leq s_i \leq v_{i,max}, \quad i = 1, \dots, N \tag{13}$$

Volume and Feature Preservation Constraints



To protect mesh quality, bound cell volumes

$$v_{i,min} \leq v_i(\mathbf{p}) \leq v_{i,max}, \quad i = 1, \dots, N,$$

where

$$v_i(\mathbf{p}) = \frac{1}{2} \sum_{j=1}^4 x_{i,j+1}y_{i,j} - x_{i,j}y_{i,j+1}, \quad i = 1, \dots, N$$

Replace cell volumes by slack variables

$$v_i(\mathbf{p}) - s_i = 0, \quad i = 1, \dots, N \tag{12}$$

$$v_{i,min} \leq s_i \leq v_{i,max}, \quad i = 1, \dots, N \tag{13}$$

Constrain all nodes on boundaries and features to preserve.

$$p_{k_i} = \hat{p}_{k_i}, \quad i = 1, \dots, n_k \tag{14}$$

14 **Problem Formulation**

Seek (u, v, p, s) satisfying

$$\min_{u,v,p,s} \frac{\alpha}{2} \|(u, v)\|_{\ell_2}^2 + \sum_{i=1}^N \sum_{j=1}^8 u_{i,j} + v_{i,j}, \quad (15)$$

subject to

$$K_i(p) - \mu_i = u_i - v_i, \quad i = 1, \dots, N, \quad (16)$$

$$v_i(p) - s_i = 0, \quad i = 1, \dots, N, \quad (17)$$

$$u_i \geq 0, \quad i = 1, \dots, N, \quad (18)$$

$$v_i \geq 0, \quad i = 1, \dots, N, \quad (19)$$

$$v_{i,min} \leq s_i \leq v_{i,max}, \quad i = 1, \dots, N. \quad (20)$$

14 **Problem Formulation**

Seek (u, v, p, s) satisfying

$$\min_{u,v,p,s} \frac{\alpha}{2} \|(u, v)\|_{\ell_2}^2 + \sum_{i=1}^N \sum_{j=1}^8 u_{i,j} + v_{i,j}, \quad (15)$$

subject to

$$K_i(p) - \mu_i = u_i - v_i, \quad i = 1, \dots, N, \quad (16)$$

$$v_i(p) - s_i = 0, \quad i = 1, \dots, N, \quad (17)$$

$$u_i \geq 0, \quad i = 1, \dots, N, \quad (18)$$

$$v_i \geq 0, \quad i = 1, \dots, N, \quad (19)$$

$$v_{i,\min} \leq s_i \leq v_{i,\max}, \quad i = 1, \dots, N. \quad (20)$$

Lemma

The starting mesh configuration lies in the feasible region, so it is nonempty!

Optimization Approach



- Utilize the **Augmented Lagrangian Sequential Quadratic Programming (ALESQP)** method (Antil, Kouri, Ridzal, 2023).
- $\mathcal{L}(x, \lambda) = f(x) + \lambda^T c(x)$
- Penalize inequality constraints, use Lagrange multipliers for equality constraints
- Requires augmented Lagrangian Hessian solves and augmented system solves

$$\begin{bmatrix} I & \nabla c(x)^T \\ \nabla c(x) & 0 \end{bmatrix} \quad (21)$$

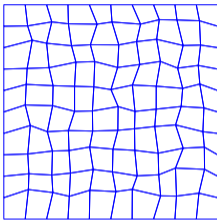
General parameters:

- Volume shrinkage/growth capped at 40%
- Optimization tolerance $1e-7$
- L2 regularization constant $a = 1$

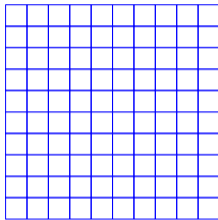
Example 1 (Perturbed uniform mesh)



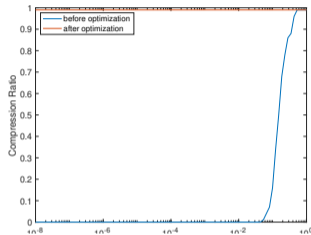
1 cluster, 1 optimization



Before



After

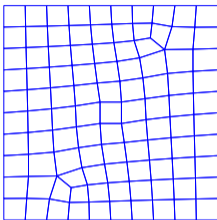


Compression

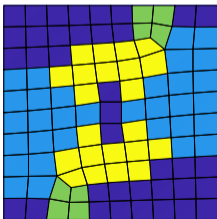
Size	AL Its	SQP Its	CG Its	$\ c(x)\ $	$\ \nabla L(x, \lambda)\ $	feas
10×10	13	34	147	$4.32e-16$	$3.99e-08$	$4.11e-10$
20×20	16	37	221	$9.10e-16$	$2.99e-08$	$1.28e-09$
40×40	500	54	447	$1.95e-15$	$1.81e-06$	$6.06e-11$

17 Example 2 (99 cell mesh)

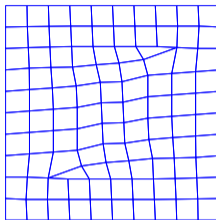
4 clusters, 2 optimizations



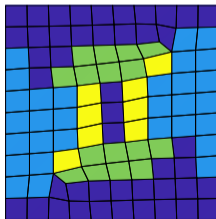
Before



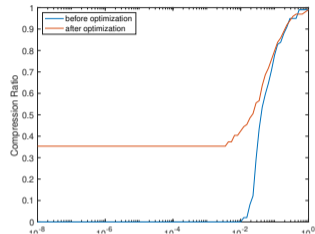
Clusters (first pass)



After



Clusters (second pass)



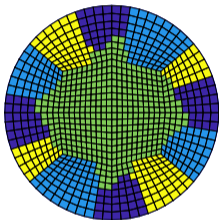
Compression

$$\begin{aligned}\|c(x)\| &= 9.05e-16 \\ \|\nabla L(x, \lambda)\| &= 6.94e-7 \\ \text{feas} &= 3.8e-9\end{aligned}$$

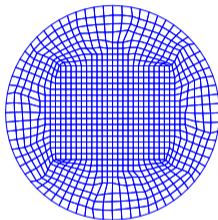
Example 3 (Circle Mesh)



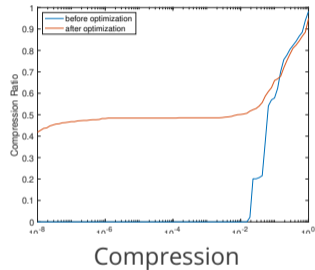
4 clusters, 1 optimization



Before



After



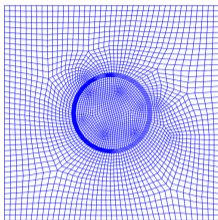
$$\|c(x)\| = 9.05e-16$$

$$\|\nabla L(x, \lambda)\| = 6.94e-7$$

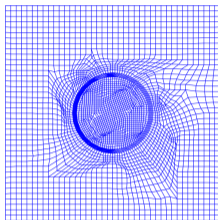
$$\text{feas} = 3.8e-9$$

Example 4 (Electromagnetics Straw)

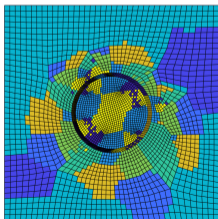
10 clusters, 2 optimizations, preserve annular "straw"



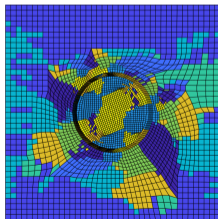
Before



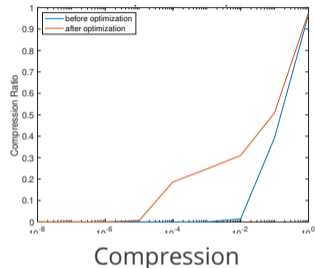
After



Clusters (first pass)



Clusters (second pass)



$$\|c(x)\| = 1.43e-10$$

$$\|\nabla L(x, \lambda)\| = 1.74e-1$$

$$\text{feas} = 3.71e-3$$



- Finite element basis compression allows for significant speedups
- Mesh optimization allows for even more speedups
- Approach is still not fully “automatic”
- Future studies on scalings, rotations, and discretization error



- Finite element basis compression allows for significant speedups
- Mesh optimization allows for even more speedups
- Approach is still not fully “automatic”
- Future studies on scalings, rotations, and discretization error

Thank you!



Why are the Jacobians equal for two cells which are translations?
Derivatives of constants are zero.

$$\begin{aligned}\Phi_1(\hat{x}) &= \begin{bmatrix} a_1 + b_1\hat{x} + c_1\hat{y} + d_1\hat{x}\hat{y} \\ a_2 + b_2\hat{x} + c_2\hat{y} + d_2\hat{x}\hat{y} \end{bmatrix} \\ \Phi_2(\hat{x}) &= \begin{bmatrix} u + a_1 + b_1\hat{x} + c_1\hat{y} + d_1\hat{x}\hat{y} \\ v + a_2 + b_2\hat{x} + c_2\hat{y} + d_2\hat{x}\hat{y} \end{bmatrix} \\ \nabla\Phi_1 &= \nabla\Phi_2\end{aligned}$$

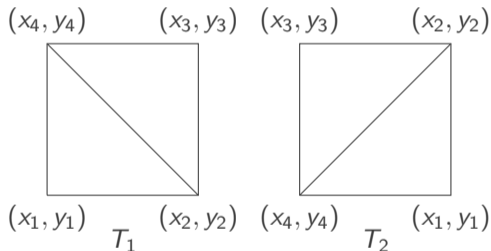
For quadrilaterals, it's easy to see

$$\Phi(\hat{x}) = \begin{bmatrix} x_1 + (x_2 - x_1)\hat{x} + (x_4 - x_1)\hat{y} + (x_1 - x_2 + x_3 - x_4)\hat{x}\hat{y} \\ y_1 + (y_2 - y_1)\hat{x} + (y_4 - y_1)\hat{y} + (y_1 - y_2 + y_3 - y_4)\hat{x}\hat{y} \end{bmatrix}$$



What about local cell orientations?

Local cell orientations are important. To keep things simple, we use a “lower-left” cell orientation scheme; however, it should only impact compression by a factor of 4.



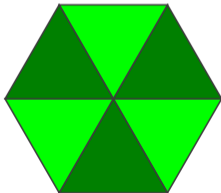
Squares with differing local node orderings



Why not use triangles?

Pros: triangles have constant Jacobians, require less data.

Cons: triangle meshes tend to have more variance in vertex degree, are less amenable to synergistic techniques like sum factorization, and a triangular plane tiling does not place similar shapes near each other.





Visualization of matches

